



Article

Cite this article: Ekaykin AA, Lipenkov VYa, Tebenkova NA (2023). Fifty years of instrumental surface mass balance observations at Vostok Station, central Antarctica. *Journal of Glaciology* 1–13. <https://doi.org/10.1017/jog.2023.53>

Received: 29 November 2022

Revised: 10 April 2023

Accepted: 3 June 2023

Keywords:

Antarctica; instrumental observations; snow density; surface mass balance; Vostok station

Corresponding author:

A. A. Ekaykin; Email: ekaykin@aari.ru

Fifty years of instrumental surface mass balance observations at Vostok Station, central Antarctica

Alexey A. Ekaykin^{1,2} , Vladimir Ya. Lipenkov¹  and Natalia A. Tebenkova^{1,2}

¹Climate and Environmental Research Laboratory, Arctic and Antarctic Research Institute, St Petersburg, Russia and ²Institute of Earth Sciences, St Petersburg State University, St Petersburg, Russia

Abstract

We present the surface mass balance (SMB) dataset from Vostok Station's accumulation stake farms which provide the longest instrumental record of its kind obtained with a uniform technique in central Antarctica over the last 53 years. The snow build-up values at individual stakes demonstrate a strong random scatter related to the interaction of wind-driven snow with snow micro-relief. Because of this depositional noise, the signal-to-noise ratio (SNR) in individual SMB time series derived at single points (from stakes, snow pits or firn cores) is as low as 0.045. Averaging the data over the whole stake farm increases the SNR to 2.3 and thus allows us to investigate reliably the climatic variability of the SMB. Since 1970, the average snow accumulation rate at Vostok has been $22.5 \pm 1.3 \text{ kg m}^{-2} \text{ yr}^{-1}$. Our data suggest an overall increase of the SMB during the observation period accompanied by a significant decadal variability. The main driver of this variability is local air temperature with an SMB temperature sensitivity of $2.4 \pm 0.2 \text{ kg m}^{-2} \text{ yr}^{-1} \text{ K}^{-1}$ ($11 \pm 2\% \text{ K}^{-1}$). A covariation between the Vostok SMB and the Southern Oscillation Index is also observed.

1. Introduction

The mass loss of the Antarctic ice sheet (AIS) is projected to be a major contributor to sea level rise (SLR) by the end of the 21st century and beyond (Meredith and others, 2019; Frederikse and others, 2020; Slater and others, 2020). Although the models predict overall ice mass loss amid continuing global warming, they also suggest an increase in the snow accumulation rate in the interior of Antarctica as a result of the increased air temperature (Frieler and others, 2015; Medley and Thomas, 2019), thus partly reducing the rate of the SLR due to shrinking of the AIS.

The ice sheet mass balance is the difference between total mass gain (net snow accumulation) and total mass loss (surface and basal ice melt and iceberg calving at the margins of the ice sheet). In turn, the net snow accumulation in the interior of the AIS results from the bulk accumulation (snow precipitation and wind redistribution) and ablation (sublimation and wind erosion) processes at the snow–air interface. The term ‘surface mass balance’ (SMB) is also used in this article as a synonym for ‘net accumulation’, as widely accepted in the literature (Eisen and others, 2008).

Although accurate instrumental snow precipitation measurements in central Antarctica are a technological challenge (Del Guasta, 2022), the SMB can be relatively easily obtained over a substantially long time interval (usually 1 year) with the use of snow height observations at stake farms or profiles. Such instrumental SMB measurements are, however, scarce in central Antarctica because they require substantial human labour and are therefore confined largely to the vicinities of the Antarctic's permanently operating stations (Table 1). For this reason, evaluation of Antarctica's SMB mainly relies upon regional climate models (e.g. van Wessem and others, 2018; Agosta and others, 2019; Mottram and others, 2021, Dumire and others, 2022), even though these model predictions often suffer from significant biases (Richter and others, 2021).

Another important source of information about the SMB variability in the recent and remote past is snow pits and firn/ice cores (Thomas and others, 2017). The interpretation of core-based SMB data might be challenging due to several reasons. Firstly, in central Antarctica, the accumulation rate observed at a single point is subject to significant random variability (‘depositional noise’). This leads to a very low signal-to-noise ratio (SNR), which prevents the reliable reconstruction of SMB climatic variations with high temporal resolution. Secondly, due to wind erosion, a fraction of annual layers are missed in the firn/ice column. Thirdly, it is not obvious for which area the results obtained from a given core are representative. Therefore, it is crucial that the investigation of the SMB based on core studies is accompanied by instrumental measurements of the snow accumulation near the core drilling site.

The first instrumental SMB observations in central Antarctica were established in 1958 at the South Pole and in the vicinity of Vostok Station. Since 1958, at least five different stake arrays have been operated at the Amundsen-Scott Station using different measurement protocols (Lazzara and others, 2012). The reference stake farm that is currently operating was installed in August 1963. Instrumental SMB measurements have also been performed at



Table 1. The main characteristics of the accumulation-stake farms in central Antarctica

Site	Coordinates, deg		Elevation, m a.s.l.	Period of operation	N of stakes	Distance between stakes, m	Size of the stake farm, m	Periodicity of observations	Acc. rate, kg m ⁻² year ⁻¹	Ref.
	Lat (S)	Long (E)								
Amundsen-Scott (South Pole)	90		2835	1963 – present ^a	50	3	50 × 25	Monthly	85	Lazarra and others (2012)
Dome Fuji	77.317	39.703	3810	1995–2012	36	20	100 × 100	Twice monthly to annually	27.3	Kameda and others (2008)
Old Dome C	74.65	124.17	3240	1975–1979	78	25	1000 × 1000	Twice, in 1978 and 1979	38	Petit and others (1982)
Concordia (Dome C) ^b	75.12	123.32	3235	2004 – present	50	40	1000 × 1000	1–7 times a year, from Nov to Feb	27	Genthon and others (2016)
Kunlun (Dome A)	80.38	77.456	4093	2005 – present	25	20	100 × 100	Twice, in 2008 and 2009	23	Ding and others (2011)
Dome A	80.38	77.456	4093	2008 – present	49	5000	30,000–40,000	Twice, in 2011 and 2013	22.9	Ding and others (2016)
Vostok	78.465	106.835	3476	1970 – present	79 ^c	25	1000 × 1000	Monthly to annually	22.5	this work

^aMoved to another location near the Amundsen-Scott station in 1974.

^bIn the 2005/2006 summer seasons, two more similar stake farms were set up 25 km north and south from Concordia (Genthon and others, 2016).

^cIn 1970–1998, one stake was operating, but since 1999, two identical farms were in use with the total of 158 stakes.

Dome Fuji Station (Kameda and others, 2008), at the old Dome C site (Petit and others, 1982), near Concordia Station (Genthon and others, 2016) and around Kunlun Station (Dome A; Ding and others, 2011, 2016); see a brief summary in Table 1.

These works made it possible to obtain reliable values of mean snow accumulation rate for the corresponding sites and, in some cases, to estimate the uncertainties of these values. On the other hand, most of these studies lack a comprehensive analysis of the SNR of the obtained SMB records.

Here, we present a review of the SMB observations at the inland Antarctic Vostok Station (78.465 °S and 106.835 °E, 3476 m a.s.l.). The Vostok SMB time series is unique in several ways. Firstly, it is the longest instrumental SMB record in central Antarctica (53 years, since 1970) obtained with a uniform technique. Secondly, Vostok Station is located within an area where the ice sheet floats on the surface of the subglacial Lake Vostok (Popov and Masolov, 2007). Due to this, the glacier surface is extremely flat here (Shen and others, 2022), which implies that the spatial SMB variability is reduced and, consequently, the observations made at Vostok are representative of a wide area around the station. The Vostok SMB data are therefore ideally suited for testing the snow accumulation rates produced by the models (Richter and others, 2021). Finally, the snow accumulation rate at Vostok is the lowest in central Antarctica, outside blue ice areas and erosion zones of mega-dunes. This is likely because this region of Antarctica is the most distant from a moisture source (Vladimirova and others, 2015). The latter probably also makes the low SMB at Vostok more sensitive to climate variability than in the other Antarctic locations, because the relative changes in saturation vapour pressure with temperature are greater in cold (and dry) air than those in warm (and humid) air.

The snow accumulation rate at Vostok has been previously addressed in a number of publications.

In the study by Barkov and Lipenkov (1978), the first statistical analysis of the stake farm data for the 1970–1973 period was performed, and the first estimates of mean annual snow build-up, surface snow density and snow accumulation rate values were produced (0.068 m, 330 kg m⁻³ and 22 kg m⁻² yr⁻¹, respectively). It was argued that the parameters of the stake farm (number of stakes and the length of the profiles) were close to optimal in terms of the uncertainty of the obtained SMB values and the required efforts.

The spatial distribution of the snow build-up across the stake farm was investigated by Ekaykin and others (1998, 2019). It was demonstrated that within the studied area, there was no

spatial trend in the mean snow build-up. At the same time, there was a very large random scatter of snow build-up values at individual stakes in a given year due to interaction of wind-driven snow with the micro-relief forms. Superimposed on this random scatter there were weak low-amplitude waves (with wavelength of about 400 m) whose contribution to the total dispersion of the build-up values over the stake farm was very small. The relationship between spatial and temporal variability of the snow build-up was also discussed. In particular, it was noted that the random scatter of the snow build-up because of snow micro-relief produced a substantial amount of ‘depositional noise’ in a time series of snow accumulation when observed at a single point (at a stake or in a snow/firn pit or core).

In the study by Ekaykin and others (2002), glaciological data collected from eight snow pits were used to reconstruct the snow accumulation rate from 1944 to 1998. A comparison of this time series with that obtained at the stake farms demonstrated a good correspondence of the mean SMB values produced by stratigraphic observations in pits and by instrumental measurements.

Vladimirova and others (2015) investigated the spatial variability of the SMB in a wider area around Vostok station with the use of the data obtained during scientific glaciological traverses. It was demonstrated that low snow accumulation values (22–23 kg m⁻² yr⁻¹) were characteristic for an area extending at least 80 km southwest and 110 km north-west of Vostok. Low SMB values (<25 kg m⁻² yr⁻¹) were typical for the whole southern half of Lake Vostok plain up to about 150 km north of Vostok. About 35 km east of Vostok, there is a mega-dune area (Ekaykin and others, 2016) where the spatial distribution of the SMB is highly disturbed.

In the study by Richter and others (2021), mean monthly and annual SMB values obtained at the Vostok stake farms were used to test the ability of Regional Atmospheric Climate Model (RACMO) and Modèle Atmosphérique Régional (MAR) regional climate models to reproduce the temporal variability of the snow accumulation rate in this region of Antarctica. The results showed that RACMO estimates of the annual and multi-year SMB agreed well with the observations, while SMB simulations by MAR were affected by a positive bias. None of the models were capable of reproducing the seasonal distributions of SMB and precipitation.

This article is devoted to a comprehensive analysis of the vast array of data on snow accumulation collected at the Vostok stake farm over the past five decades. For the first time, we present in detail the methods and protocols of instrumental SMB

measurements at Vostok and the corresponding instrumental errors (Section 2). We then rigorously assess the uncertainty in the SMB observations related to the random scatter of snow build-up values at individual stakes (Sections 3.1–3.3). The seasonal and interannual variability of the SMB at Vostok is then presented (Sections 3.4 and 3.5). The parameters of the Vostok stake farm and the protocol of snow build-up and density measurements are discussed in terms of the uncertainty of the obtained SMB values and the required efforts (Section 4.1). We then compare the instrumental SMB time series to that obtained with the use of stratigraphic investigations in snow pits and discuss the implications of the results of this work for firn and ice core studies (Sections 4.2 and 4.3). The last part of the article is devoted to the discussion of the possible drivers of the climatic variability of the SMB in the Vostok region (Section 4.4).

2. Methods

2.1. Description of Vostok's stake farms

Vostok station is located in the south-eastern corner of the Lake Vostok valley. The surface of the glacier here is flat, with the elevation gradually increasing from south-west to north-east with a slope of about 1.09 m per 1 km (Fig. 1). A detailed Global Navigation Satellite System (GNSS) survey performed in the area of the stake farm in January 2015 (Ekaykin and others, 2019) confirmed an extreme flatness of the snow plain: no relief forms larger than 100 m and/or with the height amplitude of more than 0.05 m were detected. The only exception is the route of the logistic traverses which have delivered fuel and heavy cargoes to Vostok Station every year since 1957, which is elevated above the surrounding terrain by 0.5–1.0 m (Fig. 1).

Routine observations of SMB began at Vostok Station in January 1958. Firstly, measurements were performed with the aid of an L-shaped rope profile stretched over the surface of the snow, with dimensions of 20 × 20 m and a distance between measurement points of 1 m. Observations were carried out on a monthly basis until December 1978. The obtained annual accumulation rates were proved to be unrepresentative for the Vostok area because of the small size of the profile and the short distance between the measurement points (Barkov and Lipenkov, 1978), and thus, they have not been used in the present study.

In January 1970, an accumulation stake farm was installed about 1 km north of Vostok Station (Barkov and Lipenkov, 1978). This cross-shaped farm had two 1-km long profiles oriented roughly in north-south and west-east directions (Fig. 1). Each profile consisted of 40 stakes set up at 25 m intervals with the central stake (n_{20}) common for both profiles (79 stakes in total).

The stake farm was visited once a year, in late December, to measure the stakes' heights and the density of the upper layer of snow. In certain years (1970–1993, 1995, 2004 and 2006), the measurements were carried out on a monthly basis.

As seen in Fig. 1, this stake farm is crossed (between stakes n_{69} and n_{70}) by the logistic traverse route. The snow surface and thus the snow accumulation field have become disturbed in the close vicinity of it.

On 29 December 1998, a new stake farm was set up to the west of the old one in such a way that the west-east profiles of both farms formed a single 2 km profile (Fig. 1). The parameters of both farms (shape, number of stakes and distances between them) are identical, with the only difference being the material used for the stakes: aluminium poles are used at the old farm and bamboo sticks at the new one. The new stake farm is located in a clean area not affected by the traverse route or other artificial objects, so the parallel observations at the two farms have allowed us (1) to confirm the validity of the SMB data obtained from the

old stake farm and (2) to assess the representativity of the measurements performed at the 1 km² test area.

In December 2003, the stake farms were not visited, and so only the mean annual snow accumulation is available for the years 2003 and 2004.

By 2005, the poles at the old farm became almost completely buried under the snow. They were therefore re-installed and re-measured to preserve the continuity of the record.

In December 2019, construction of a snow foundation for a new Vostok wintering complex began, and anthropogenic activity on the logistic route and in the area to the west of the old Vostok Station increased considerably. In connection with this, on 29–31 December 2019, the old stake farm was moved south–south–east, to a new location behind the station's air strip (AS). It was named the 'AS stake farm' (Fig. 1). The time series of the SMB observations at the old farm thus finished in December 2019, and starting from 2020, observations were continued both at the AS stake farm and at the new stake farm left at its original location, which has ensured the integrity of the historic SMB record at Vostok.

2.2. Snow build-up measurements

The SMB during a given period of time is obtained as the product of the snow build-up and the density of the accumulated layer measured at the end of this period (Eisen and others, 2008). Snow build-up at a stake is observed as the difference between the stake's height above the snow surface at the beginning and at the end of the observation period. Despite the apparent simplicity, there are several sources of uncertainty associated with this method of measuring snow build-up.

Firstly, the stake's base can move vertically relative to the snow layer in which it was initially installed. The stake may either sink or emerge, thus increasing or decreasing apparent snow build-up. Sinking may happen due to the melting of the snow layer below the stake (if the stake is made of heat-conducting material such as aluminium) or because of the stake's vibration driven by wind activity. The stake may emerge if it gets stuck in a snow layer bedded between the stake's base and the snow surface. To avoid vertical displacement of a stake, one may firmly anchor (fasten) the stake's base to the layer of snow that contains it. At Vostok, the stakes are not anchored, but during installation, they were pushed into the snow until their bases became stuck in a hard snow layer, thus preventing them from sinking. The old Vostok stake farm is made of aluminium poles (Fig. 2), while the new one consists of bamboo poles.

Secondly, the snow surface is uneven, so the stake's height depends on the side along which the stake is measured. We estimate a typical error related to this irregularity as ± 0.01 m, and the error of snow build-up (the difference of two stake height measurements) is ± 0.014 m or about 23% of the mean annual snow build-up at Vostok. It could be decreased by measuring the height along four sides of a stake and then taking the average. However, this additional effort would not improve the accuracy of the SMB measurements significantly, because, as shown below, the standard deviation (SD) of the annual snow build-up at an individual stake amounts to 100% of its mean value for the whole stake farm. During multi-year observations, the random error related to the snow surface roughness remains almost constant. Therefore, its contribution to the overall uncertainty of the multi-year mean snow build-up at a single stake decreases as the observation period increases.

Finally, the snow build-up measured with the aid of the accumulation stakes is systematically underestimated due to the compaction of the snow layer between the stake base and the snow surface (Ekaykin and others, 1998; Takahashi and Kameda, 2007; Eisen and others, 2008). The impact of this effect depends on the snow density profile, i.e. on the vertical gradient of the

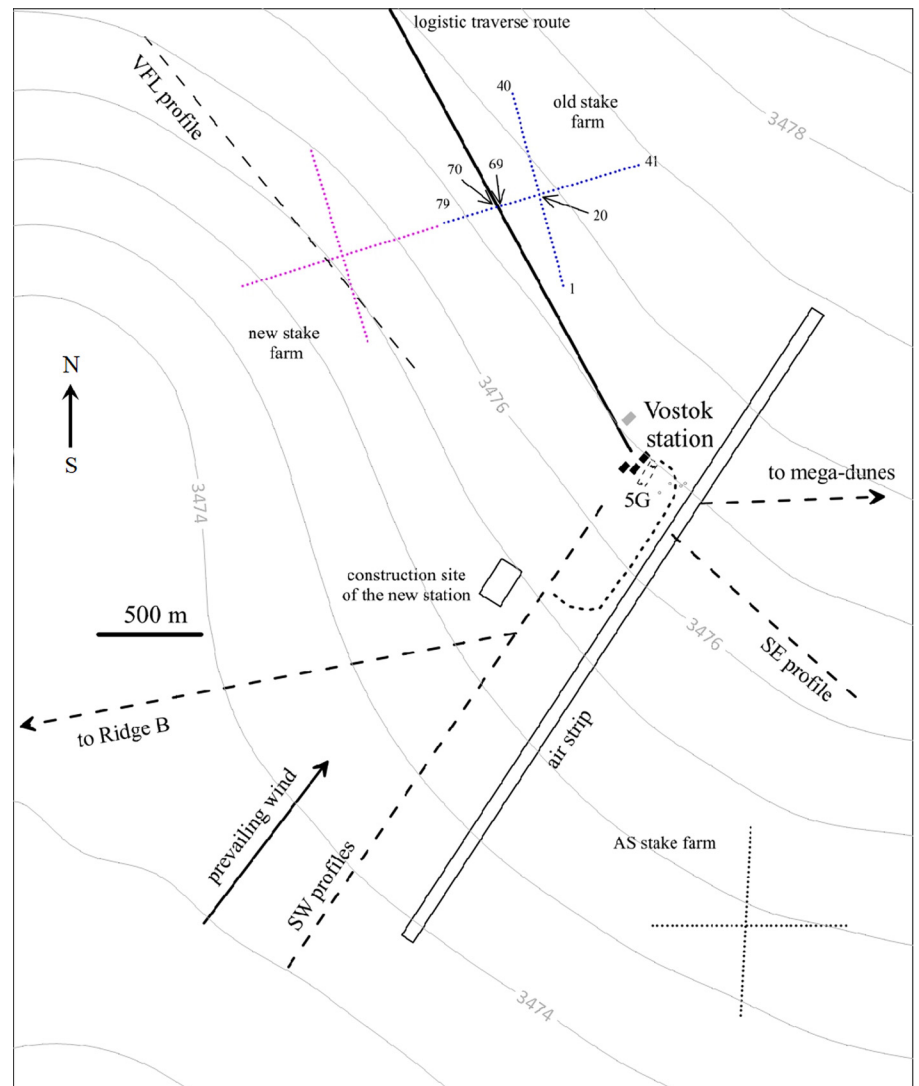


Figure 1. The location of the accumulation stake farms in the vicinity of Vostok Station. The dots depict the positions of the stakes of the old farm (blue), the new farm (magenta) and the AS farm (black). For the old farm, the numbers of selected stakes are shown: 1, 40, 41 and 79 are the extreme stakes of the farm, stake 20 is the central one, and stakes 69 and 70 are the closest to the logistic traverse route. Also shown are the logistics route from Vostok to Progress Station (bold solid line), air strip (long rectangle), the construction site of the new Vostok wintering complex (small rectangle), routes of scientific traverses and glaciological profiles (dashed lines with and without arrows) as well as the prevailing wind direction and south-north direction. Isohyps depict the ice surface elevation above WGS84 according to DiMarzio and others (2007).

snow density and the depth of the stake base. There are several approaches to derive the correction for the snow compaction (see the review in the study by Ekaykin and others (2020)). Firstly, the correction can be calculated if the vertical snow density profile is known with sufficient accuracy, assuming it does not change with time (Sorge, 1935). Secondly, the snow compaction can be measured instrumentally. Thirdly, the correction can be obtained by comparing the SMB values from the stake farm with the ones derived from independent studies (e.g. from snow pits or shallow core studies). At Vostok, the true annual snow build-up is $8 \pm 4\%$ higher than the observed build-up due to the effect of snow compaction (Ekaykin and others, 2020).

2.3. Snow density measurements

Snow density is measured at the Vostok stake farms with the aid of the VS-43 sampling device (Ismagilov and others, 2018), which is routinely used in Russian glaciological practice (Fig. 2). The probe is equipped with a steelyard, which allows us to measure the mass of the sampled snow of the known volume on the spot where the sample was taken.

In the case of low-accumulation sites like Vostok, the annual snow build-up does not represent a spatially continuous layer, but rather separate patches of snow varying in size and thickness. Thus, determining the density of the recently deposited annual layer of snow is not straightforward at Vostok. Even greater difficulties of the same nature arise when estimating the monthly values of the SMB.

In view of these complications, we adopted a rule to measure the density of the upper 0.20 m layer of snow near every fifth stake on each of the Vostok stake farms. The sampling depth of 0.20 m and the number of sampling points (18 density datapoints at each stake farm) were chosen as a trade-off between the required efforts and the accuracy of the obtained results. The accuracy of a single measurement with the VS-43 for the upper 0.20 m of snow is about 9–10 kg m⁻³, i.e. about 3% of the average surface snow density at Vostok.

The mean snow density measured at the end of the year (in December) is used to calculate the annual accumulation of snow at each stake farm, whereas the mean monthly values are used to investigate seasonal variations of the near-surface snow density.

3. Results

As a result of glaciological works at the Vostok stake farms, a SMB database was created that contains >22 000 individual values of monthly snow build-up, about 5600 values of annual snow build-up and >5600 values of snow density. In this section, we first analyze these data array to understand if the build-up measurements at individual stakes are independent or there is 'noise correlation' at adjacent stakes. Then we describe the spatial scatter of the monthly and annual values of snow build-up and density, and investigate how the error of the mean build-up depends on the number of measuring points and period of observation. Finally, we consider data on the seasonal and interannual variability of the snow build-up, density and accumulation rate.

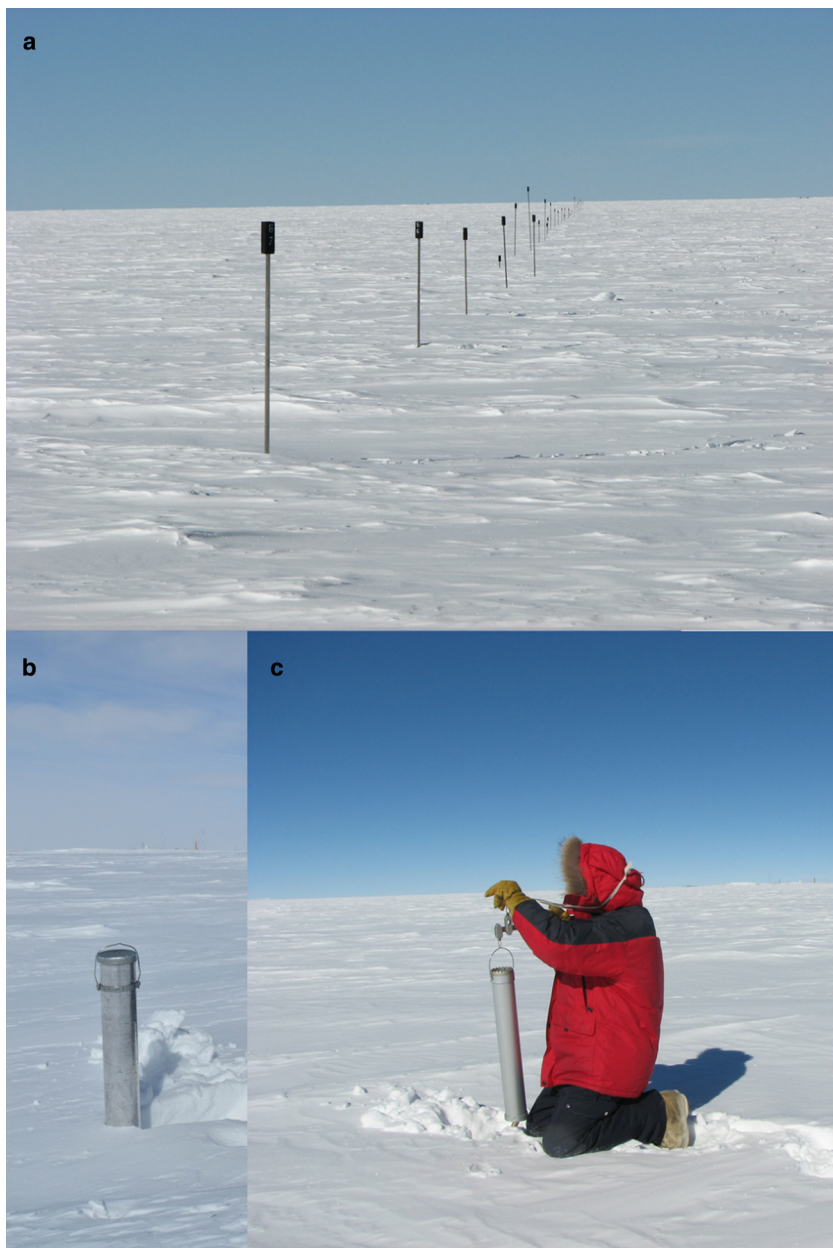


Figure 2. North-south profile of the old stake farm (a) and the process of the snow density measurement with the use of VS-43 device (b and c).

3.1. Independence of the snow build-up values at adjacent stakes of the farm

Before performing a statistical analysis of the build-up data, it is necessary to make sure that the build-up values obtained at neighbouring stakes of the farm are independent. Indeed, if the distance between stakes is smaller than the horizontal size of the snow micro-relief forms, then the time series of snow build-up measured at adjacent stakes may contain the same 'depositional noise'. To check if the distance between stakes at Vostok stake farms is large enough to avoid such noise correlation, we compared the mean correlation coefficients, $\langle R \rangle$, between the time series of the annual build-up obtained in 1970–2019 at the old stake farm at the adjacent stakes (set up at a 25 m interval) and at the stakes separated by 50 m or more.

We found that in the former case (77 pairs of time series), $\langle R \rangle = 0.071$, whereas in the latter case (3003 pairs of time series), $\langle R \rangle$ decreases to 0.043. Although small, both of the coefficients are statistically significant because of the great number of time series involved. The difference between them is, however, not significant, which allows us to conclude that the 25 m distance between

stakes is large enough to avoid spatial correlation between neighbouring measurements.

A similar analysis performed on 77 pairs of generated random series gives $\langle R \rangle = 0.001$ and a very low likelihood ($\sim 0.02\%$) of obtaining $\langle R \rangle = 0.07$. This test confirms that in the time series of the annual snow build-up obtained at individual stakes, there is a small fraction of variance common to all the time series, which most likely represents a climate signal.

Another approach to examine interstake correlation is to use the so-called structural function (Barkov and Lipenkov, 1978; Eisen and others, 2008). Its application leads us to the same conclusion: the measurements of annual snow build-up at the adjacent stakes at the Vostok stake farms are independent.

3.2. Spatial scatter of snow build-up and density

The dataset on the monthly snow build-up at the old stake farm contains 22 345 individual values. This array demonstrates extremely high scatter of the values: the minimum and maximum extremes at individual stakes are, correspondingly, -0.295 and

+0.33 m, with the mean monthly build-up equal to +0.0051 m. This scatter contains both spatial variations (between individual stakes in the same month) and temporal variations (climatic variability of snow build-up from month to month). To extract the spatial component of the total variance, we calculated the anomalies of monthly values of snow build-up for each stake (i.e. the difference between the build-up value at an individual stake and the farm-average value in a given month). The distribution of these anomalies is presented in Fig. 3a. We also calculated the anomalies of annual build-up values (Fig. 3b), as well as the anomalies of snow density values (Figs 3c and d).

The absolute magnitude of the monthly build-up anomalies is nearly 0.63 m, but 75% of the datapoints fall into the $-0.025 \dots +0.015$ m bin (Fig. 3a), and most of the values (92.5%) lie in the range between -0.045 and $+0.045$ m. The SD is 0.0293 m. In general, the distribution of the monthly build-up values is similar to Gaussian distribution but with an increased likelihood of large negative and positive anomalies (<-0.1 and $>+0.1$ m). The coefficient of variation ($CV = SD/\text{mean}$) of the monthly build-up values is 5.7.

For the annual build-up values at the old farm in 1970–2019, the average value is +0.061 m, and the minimum and maximum extremes are -0.37 and $+0.38$ m, respectively. The distribution of the anomalies (Fig. 3b) has a clear right-side asymmetry, which can be attributed to nonuniform redistribution of snow by wind: the wind removes the thinner layers of snow from larger areas and deposits it in thicker layers over smaller areas. The SD of the annual build-up anomalies is 0.054 m ($CV = 0.9$), and $>95\%$ of the anomalies lie in the range between -0.095 and $+0.105$ m.

Over the common period of operation of the old and new stakes farms (1999–2019), their mean annual build-up values (0.063 and 0.067 m) are statistically undistinguishable from each other.

The large spatial scatter of the monthly and annual snow build-up values is due to the interaction of the wind-driven snow redistribution with the surface relief – mainly micro-relief forms like sastrugis, dunes, whalebacks, ripples, etc. Since the magnitude of the snow micro-relief forms (typically 0.1–1 m, Picard and others (2019)) exceeds monthly and annual snow build-up values, the snow accumulation field is highly spotty

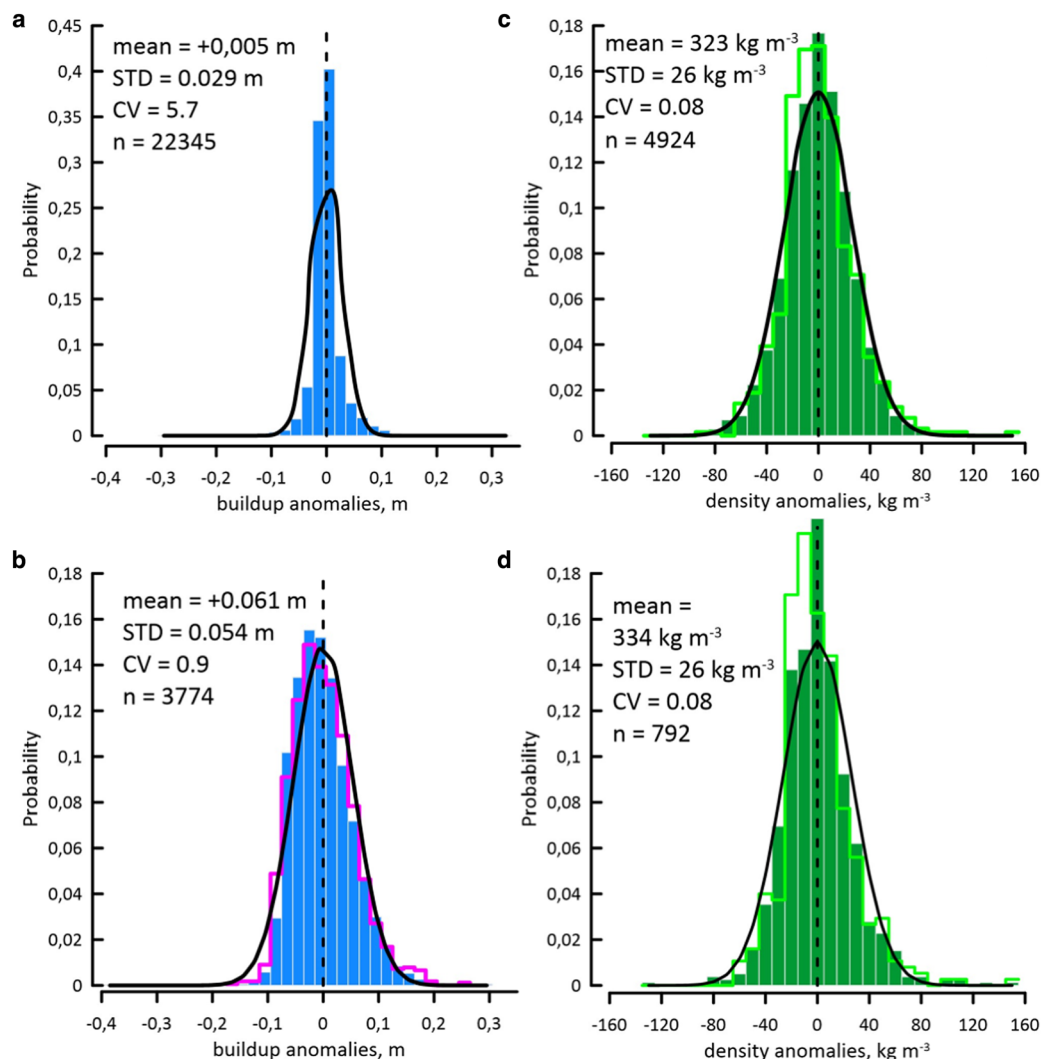


Figure 3. Spatial variability of the snow build-up and surface snow density. The histograms represent the distributions of anomalies of monthly and annual values of build-up and density for each stake (i.e. the difference between a value at an individual stake and the farm-average value in a given month or year): (a) monthly snow build-up values at the old stake farm; (b) annual snow build-up values at the old (coloured bars, 3774 measurements) and new (magenta stepped line, 1659 measurements) stake farms; (c) snow densities measured on a monthly basis at the old (coloured bars, 4924 measurements) and new (green stepped line, 637 measurements) stake farms; (d) December snow densities at the old (coloured bars, 792 measurements) and new (green stepped line, 375 measurements) stake farms; Black curves – Gaussian distribution whose mean and SD are the same as those of the experimental data. Main statistical parameters (mean, SD, coefficient of variation and number of datapoints) are given for the old stake farm. The vertical dashed lines denote 0 value.

with the increased accumulation of snow in some locations, usually in hollows on the leeward side of the dunes or sastrugis, and zero or negative accumulation in others. Such spatial variability in the snow build-up creates the so-called depositional noise in the time series of the snow accumulation as observed at a single point.

The snow densities measured in 1970–2019 on a monthly basis at the old stake farm are characterized by a mean value of 323 kg m^{-3} with the extremes of 190 and 520 kg m^{-3} . The distribution of the monthly density anomalies (Fig. 3c) closely fits a Gaussian curve with the SD of 26 kg m^{-3} . Relative variability of the density values expressed by the coefficient of variation ($CV = 0.08$) is significantly less than that of the build-up values.

Over the period of time when new and old stake farms were operated simultaneously, the mean snow density at both farms was the same (331 kg m^{-3}).

Finally, in Fig. 3d, the distributions of the anomalies of snow densities measured each December are shown. The density data arrays obtained at the old and new stake farms are statistically identical and obey Gaussian distribution with an SD of 26 kg m^{-3} . The mean December density and the full range of its scatter are, respectively, 334 and 236 – 520 kg m^{-3} at the old stake farm (period of observation is 1970–2019, 792 values in total), and 337 and 270 – 485 kg m^{-3} at the new farm (period of observations is 1999–2019, 375 values in total). The mean snow density in December is noticeably higher than the mean density based on year-round observations, which is due to the seasonal cycle of the surface snow density (see section 3.3).

A fraction of the total scatter of the snow build-up and density values is produced by the instrumental errors during the measurements of these parameters. For the snow build-up, the instrumental error is about 0.014 m (Section 2.2), so it accounts for about 23% of the total variance of the monthly values ($SD = 0.0293 \text{ m}$), while its fraction in the total variance of annual build-up values ($SD = 0.054 \text{ m}$) is only 7%. For density, the instrumental error (about 10 kg m^{-3}) accounts for about 15% of the total variance ($SD = 26 \text{ kg m}^{-3}$).

3.3. Standard error of mean snow build-up as a function of the number of stakes and period of observation

The SD of annual snow build-up, as observed at an individual stake, equals about 90% of the mean annual snow build-up at Vostok ($CV = 0.9$). It means that to obtain accurate data on the SMB, we need to carry out observations at an array of many stakes and/or over a long period of time.

As shown in Section 3.1, the build-up measurements at adjacent stakes of the farm are independent. In this case, the standard error of the mean (SEM) build-up value can be calculated as SD/\sqrt{N} , where SD is the standard deviation and N is the number of datapoints. In Fig. 4, we demonstrate how SEM depends on the number of stakes and the period of observation. When the number of stakes increases from 1 to 10, the SEM rapidly decreases by a factor of 3.5, while the further increase in the stake number results only in a small reduction in the SEM. For the whole array of 79 stakes, the SEM equals 0.006 m or about 10% of the mean annual snow build-up at the stake farm. To reduce the relative error to 5%, one would need to raise the number of stakes to 350, which will unreasonably increase both the time and the manpower needed to operate such a stake farm.

The SEM also decreases with the increase of the observation period (Fig. 4). Note, however, that the standard error of mean annual build-up obtained by measurements at a single stake over a 10-year period (0.017 m) is higher than that obtained by measurements at 10 stakes over a single year (0.016 m). This is because the interannual variability of the snow build-up at an

individual stake is a sum of both the depositional noise and the climatic variability.

The SEM calculated for 18 datapoints of the surface snow density measured in each December averages 6.3 kg m^{-3} ($CV = 0.02$). Thus, the contribution of the snow density spatial scatter to the depositional noise in the time series of annual snow accumulation is weaker than that of the snow build-up ($CV = 0.1$).

3.4. Seasonal variability of snow build-up and density

In Fig. 5, we present mean monthly values of snow build-up and density for the period from 1970 to 2019. Despite the wide error bars, the seasonal cycle is clearly visible in both parameters.

A reduced snow build-up is observed during the warm period (from November to February), while the maximum build-up values are characteristic of late winter to early spring (September–October). On the one hand, this annual course can be explained by the increased cyclonic activity in the second half of the Antarctic winter (Turner and others, 2019), which brings moisture to the interior of the East Antarctic plateau. On the other hand, the low snow accumulation in the austral summer can be attributed to radiation-enhanced sublimation. It has been demonstrated that sublimation from the snow surface summed over the warm period (November to February) amounts to 2.3 mm w.e. , or about 0.007 m in snow equivalent (Ekaykin and others, 2015). In addition, we should also take into account the wind-driven sublimation from drifting snow particles, which may well increase the overall sublimation effect (Amory and others, 2021). It thus appears that in fact the precipitation rate in summer and winter might be of similar magnitude, and the observed seasonal cycle of snow build-up is merely the result of enhanced sublimation during the warm period.

Another factor that may have an impact on the decrease in the snow build-up measurements during summer is the snow compaction. Our recent direct measurements of the snow compaction rate at Vostok (to be published elsewhere) demonstrate that much of the compaction occurs mostly in two summer months (December and January), while in the winter, the rate of compaction is several times lower.

The surface snow density demonstrates a prominent seasonal cycle, too: in midwinter, the snow is about 6% less dense than in summer. This can be explained by the increased snow build-up in the cold period (Fig. 5), which results in a higher proportion of fresh loose snow in the uppermost 0.20 m of snow during the winter. Indeed, the total winter (March–September) snow build-up amounts to about 0.045 m , or nearly $\frac{1}{4}$ of the 0.20 m layer, the density of which is measured. The density observed at the end of winter (315 kg m^{-3}) can be achieved if the density of the uppermost 0.045 m of fresh snow is 260 kg m^{-3} , and the density of the deeper 0.155 m of snow is 330 kg m^{-3} , which seems to be close to reality. This scenario assumes that the fresh winter snow is not densified until spring, which is consistent with our observation that the snow compaction occurs mostly in summer and slows down significantly in the cold part of the year.

3.5. Interannual variability of snow build-up and density

In Fig. 6, we show the time series of the mean annual snow build-up, December snow density and the accumulation rate obtained from the Vostok stake farms. The uncertainties in the data (the error envelopes in the figure correspond to 2 SEM) do not obscure the climatic signal, which is clearly seen in all the presented time series.

The correlation coefficient, R , between snow build-up records from the old and new stake farms during the time interval when they were operated simultaneously (1999–

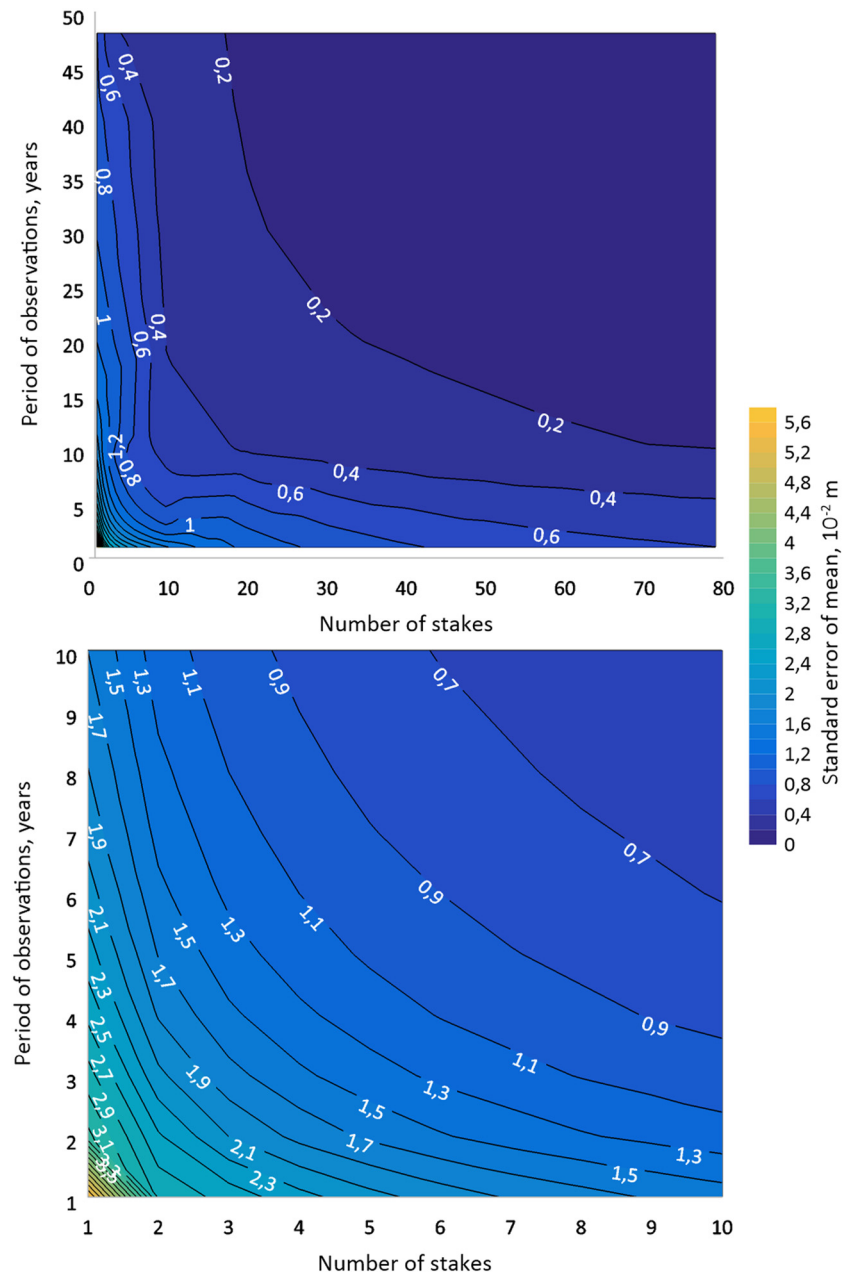


Figure 4. Standard error of the mean annual snow build-up (in 10^{-2} m) at the old stake farm as a function of the number of stakes and the period of observation. The lower panel is a zoom-in of the diagram limited by 10 stakes and 10 years.

2019) equals 0.60 ± 0.19 and is statistically significant. As for the December snow density, the correlation between the two farms is even stronger ($R = 0.75 \pm 0.16$), which can be explained by a smaller contribution of depositional noise (spatial scatter) to the interannual variations in surficial density. Consequently, the correlation between the time series of the snow accumulation rate obtained at the old and new stake farms ($R = 0.70 \pm 0.17$) is statistically significant as well. The fact that all the time series obtained at the two neighbouring stake farms are correlated confirms the significance of the observed climatic signals, which will be discussed in the next section.

The absence of correlation between snow build-up and density ($R = 0.10 \pm 0.15$) indicates that these two parameters are governed by different climatic factors. At the same time, the correlations established between snow build-up and accumulation rate ($R = 0.98$), and between accumulation rate and snow density ($R = 0.31$) suggest that more than 90% of the interannual variability of the SMB is explained by changes in the snow build-up and only <10% can be attributed to changes in snow density.

4. Discussion

4.1. Optimal parameters and representativeness of the Vostok stake farms

The uncertainty of the SMB observations depends on the three interrelated parameters of a stake farm: (1) the size of the stake farm, (2) the distance between the adjacent stakes, and (3) the number of stakes. Another source of uncertainty is the instrumental errors during the measurements of snow build-up and density.

The size of the farm must be larger than (or at least comparable to) the typical size of the snow relief forms. If the length of a stake profile is less than the wavelength of the snow dunes, then the mean snow build-up measured at the stakes would be biased relative to the true value for the studied area. The interaction between the snow surface relief and the snow build-up has been clearly demonstrated by the example of mega-dunes (Ekaykin and others, 2016). The size of the stake farms at Vostok is 1×1 km. The study of the spatial variability of the snow build-up at the stake farms revealed a strong contribution of noise related to the snow micro-

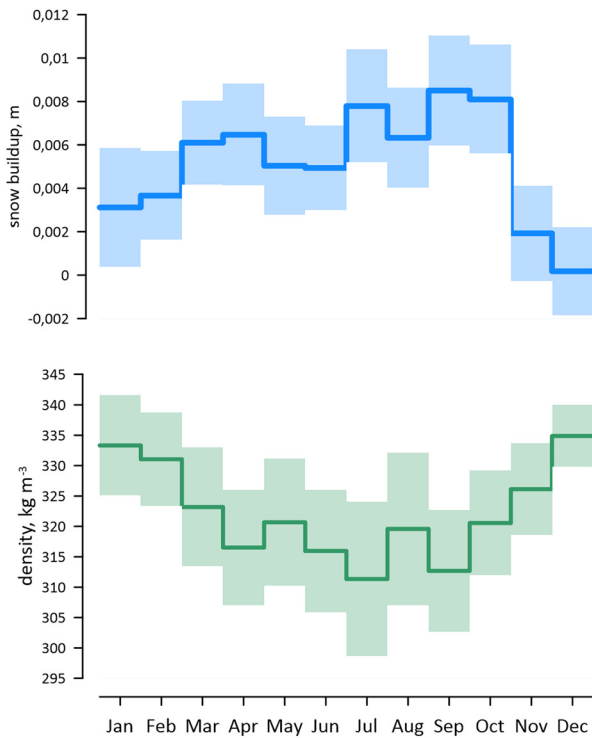


Figure 5. The seasonal cycles of snow build-up (upper panel) and density (lower panel) as revealed from the monthly measurements at the old stake farm. Error bars shown as shading represent 2 SEM.

relief forms (Section 3.2). In the study by Ekaykin and others (2019), the presence of weak low-amplitude waves (probably associated with ‘meso-dunes’ with a wavelength of about 400 m) was also suggested. We do not expect large forms of dunes (like those typical for the vicinities of South Pole (van der Veen and others, 1999; Hamilton, 2004) and Dome C (Eisen and others, 2005)) at the glacier surface near Vostok because of its extraordinary flatness, as observed in satellite images (Shen and others, 2022) and GNSS survey (Ekaykin and others, 2019).

In Section 3.3, we show that an increase in the number of stakes from 1 to 10 effectively decreases the SEM annual build-up. A further increase in the number of stakes leads only to a slow reduction of the SEM. With 79 stakes, as at the Vostok stake farms, the SEM is about 10% of the mean annual snow build-up value, which enables us to reliably resolve interannual variability of snow accumulation.

Both the old and the new Vostok stake farms can be processed within 1 working day; a larger number of stakes would require much more time and effort, with only a small increase in the accuracy of the results.

Finally, the distance between stakes (25 m) is large enough to avoid ‘noise correlation’ between adjacent stakes (Section 3.1).

The aforementioned consideration leads us to the conclusion that the parameters of the Vostok stake farms (number of stakes, distance between them and the size of the stake farm) are close to optimal for studying the SMB annually. It is not the case for the L-shaped profile that was operated at Vostok in 1958–1978 (Section 2.1): the size of the profile (20 × 20 m) is comparable with typical lengths of snow micro-relief forms (10 m), and the distance between the measuring points (1 m) is too short. The same is probably valid for the stake farm operating at the Amundsen Scott station, where the distance between stakes (3 m) is too short to avoid inter-stake correlation and the size of the array (roughly 50 by 25 m) is too small compared to the size of the snow dunes typical for this region of Antarctica (van der Veen and others, 1999; Hamilton, 2004).

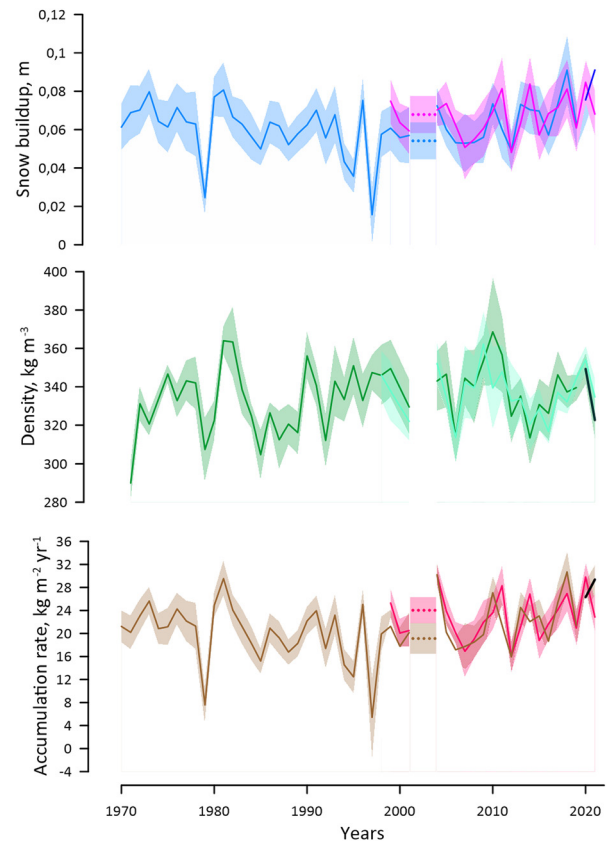


Figure 6. Interannual variability of the snow build-up (upper panel), and December snow density (middle panel) and of the resulting snow accumulation rate (lower panel). Blue, green and brown colours are used to depict data on, respectively, snow build-up, density and the accumulation rate from the old stake farm; magenta, light green and red – the same data from the new stake farm; dark blue, dark green and black – the same data from the AS farm. The shading depicts the error bars (± 2 SEM). The dotted lines show the mean values of the snow build-up and accumulation rate in 2003–2004. The build-up and the snow accumulation rate values are not corrected for the snow compaction.

As described in Section 2.1, the stakes of the old and new Vostok farms are made of different materials (correspondingly, aluminium and bamboo). However, the mean snow build-up values do not differ significantly at the two farms, and the distribution of the individual values is similar (Fig. 3). This means that the stake material has no measurable effect on the instrumental SMB observations in the conditions of Vostok station.

The contribution of the spatial and temporal variability of the surface snow density to the total variability of the SMB at Vostok is significantly less than the contribution of the snow build-up, as demonstrated in Sections 3.2 and 3.5. Even if we used a constant density value to calculate snow accumulation, it would not significantly affect the results of this study. However, as shown in Fig. 6, the interannual variability of the surficial density exhibits a clear climatic signal, so regular measurements of this parameter will help to investigate the reaction of the snow thickness properties on the environmental changes.

According to our measurement protocol, we measure the density in the upper 0.20 m of snow, while the average annual build-up is about 0.06 m (Section 3.2). The thickness of 0.20 m was chosen as a trade-off between required efforts and accuracy since the instrumental error of the density measurements strongly increases with the decrease of the sampling depth (e.g. for a 0.20-m layer, it is equal to about 10 kg m^{-3} , while for a 0.06-m layer, it is about 28 kg m^{-3}). We note here that a comparison of the mean snow density in the upper 0.06 m and in the upper 0.20 m of the snow thickness shows that the 0.20-m density is slightly higher than the 0.06-m

density (Ekaykin and others, 2020). Thus, our approach to determine the ‘effective’ density may somewhat overestimate the snow accumulation rate. However, the corresponding uncertainty of the accumulation rate is within the uncertainty of the correction related to the compaction of the snow (see Section 2.2 and Ekaykin and others, 2020).

4.2. Implications of snow stake data for ice core studies

The dataset of the SMB parameters provided by the observations at the Vostok stake farms allows us to estimate the SNR in the time series of the snow build-up and density obtained at a single point (Fisher and others, 1985):

$$\text{SNR} = \langle R \rangle / (1 - \langle R \rangle),$$

where $\langle R \rangle$ is the mean correlation coefficient between the time series from individual stakes.

In the case of snow build-up, $\langle R \rangle = 0.043$ (see Section 3.1), and $\text{SNR} = 0.045$, which means that about 96% of the variance in the snow build-up time series is explained by depositional noise and only 4% is attributed to a climatic signal. (We note that the high correlation revealed between the time series of the mean annual snow accumulation rates at the old and new stake farms ($R = 0.70$) results in an enhanced SNR (2.3).)

Due to the highly uneven snow deposition, the time series of any properties of snow/firn/ice thickness (e.g. isotopic and chemical composition) obtained at a single point contain a substantial amount of noise, thus making extraction of high-resolution information on climatic conditions from firn and ice cores drilled in low-accumulation areas of central Antarctica difficult. However, the SNR values for some properties may differ from that for the snow build-up. For example, the SNR for the stable water isotope composition is higher than for the snow accumulation because the diffusion of the water molecules in firn tends to suppress the high-frequency noise in the isotopic record (Fisher and others, 1985).

The data presented in Section 3.2 can be used to calculate the probability of the annual layer hiatus in studied snow pits and firn or ice cores. The number of annual build-up observations at individual stakes with values equal or less than 0 m is 13.7% of the total number of observations at the old stake farm and 11.7% at the new one. One can argue that if an annual snow layer is thin enough (~ 0.01 m), then in the course of snow metamorphism, its boundaries would disappear, thus making it undistinguishable from a neighbouring layer. By using 0.01 m as a cut-off value, we obtain $19 \pm 2\%$ as the best estimate of the probability of annual layer hiatus in present-day conditions at Vostok, while noting that the hiatus probability inversely depends on the snow accumulation rate. A similar result was obtained when studying the snow stratigraphy in eight snow pits investigated in the vicinity of Vostok (Ekaykin and others, 2002). In each snow pit, the depths of 1955 and 1965 radioactive reference layers were defined, and the number of snow strata between these layers and the snow surface was counted. It was established that on average the total number of stratigraphic layers in a snow thickness is 18% less than the actual number of years during which this thickness has been deposited.

A time series of the snow build-up obtained from a snow pit or firn core substantially differs from that obtained by instrumental measurements at a stake farm. In the case of snow removal by wind, the underlying snow layer is eroded and becomes thinner. For example, at stake 7 of the old farm, the following sequence of build-up values was observed in 1986–1993: +0.125, +0.07, −0.01, +0.025, +0.045, +0.07, −0.165 and +0.33 m. If one excavated a pit near this stake, in its stratigraphic section, this

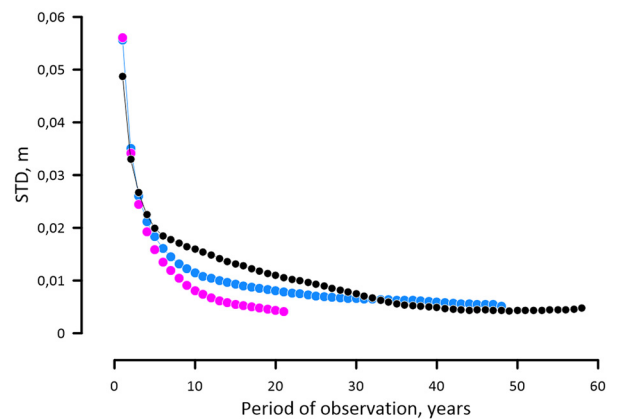


Figure 7. The uncertainty (SD) of the mean annual build-up values obtained at individual stakes as a function of the observation period for the old (blue) and new (magenta) stake farms. The black line depicts the same function defined with the use of data from eight snow pits (Ekaykin and others, 2002).

sequence would be represented by the layers from 1985 and 1986 (0.125 and 0.35 m) overlaid by thick (0.33 m) layer from 1993, while five annual layers (1988–1992) would be missed. Note that in this example, the average thickness of these snow layers (if we do not take into account missed annual layers) is 0.163 m, while the real average snow build-up in this point in 1986–1993 was 0.061 m. Due to this effect, the average thickness (reduced to the surface snow density) of annual snow layers defined as a result of stratigraphic observations in snow pits is about 18% larger than the real mean annual snow build-up.

In Fig. 7, we plotted the SD of the mean annual build-up values obtained from individual stakes as a function of the observation period. The graphs in this figure can be used for estimating the standard error of the SMB measurements derived from snow pits and cores. For example, the mean snow accumulation rate derived from a single core for a 30-year time period would have a standard error of about 0.066 m yr^{-1} in snow equivalent or about $22 \text{ kg m}^{-2} \text{ yr}^{-1}$ in mass.

Note that the SD of the mean annual build-up values at the old stake farm is systematically higher than at the new one. This can be explained by the disturbance of the snow accumulation field caused by the presence of a logistical route passing through the old farm (Fig. 1): due to snow re-distribution by wind, the snow build-up is reduced windward from the route and elevated leeward from it (Ekaykin and others, 2019). The snow redistribution affects several stakes nearest to the route, but does not affect the mean snow build-up averaged over all the stakes, as is evident by comparing data from the old and new stake farms (Section 3.2).

In Fig. 7, we also show the SD of mean snow accumulation (reduced to the surface snow density) as a function of the observation period, as defined with the use of the data from eight snow pits (Ekaykin and others, 2002). We note that the curves for pits and for stake farms are comparable, especially for longer periods of observation.

In general, the analysis of the instrumental snow build-up data obtained at the stake farm may contribute to the interpretation of SMB datasets extracted from snow pits or firn/ice cores. Firstly, a number of missed annual layers can be estimated in case if this information is not available otherwise. Secondly, the data presented in Sections 3.2 and 3.3, and in Fig. 4, may help to estimate the number of records (pits or cores) required to obtain the SMB values with a desired uncertainty. Thirdly, the data presented in Fig. 7 can be used to estimate the degree of smoothing required to reduce the depositional (stratigraphic) noise to a desired level.

4.3. Comparison of stake-derived SMB values with data from snow pits

Given the fact that the time series of snow accumulation rate obtained at the old and new stake farms are well correlated with each other, we can construct a composite accumulation rate record for the period 1970–2021 using the data from all three Vostok stake farms. From 1970 to 1998, our Vostok composite record consists only of the data from the old stake farm, while from 1999 to 2019, it is represented by the mean accumulation rate at the old and new stake farms, and from 2020 to 2021, it is represented by the mean accumulation rate at the new and the AS stake farms. To eliminate bias due to snow compaction, we added $1.66 \text{ kg m}^{-2} \text{ yr}^{-1}$ (Ekaykin and others, 2020) to each annual value of the snow accumulation rate. Strictly speaking, the correction for the snow settling is not constant because the depth of the stakes' bottom gradually increases with time. However, this has a little effect on the correction since the snow density changes insignificantly in the 0.5–3 m depth interval (Ekaykin and others, 2020). We also note that the interannual variability of the correction does not exceed its error, which is estimated to be as much as 50% (Ekaykin and others, 2020).

The resulting annually resolved record of the SMB is shown in Fig. 8b alongside with the stacked record of the snow accumulation rate in 1944–1998, which was derived from stratigraphic studies in eight snow pits (Ekaykin and others, 2002). Although

in their overlap period (1970–1998), the two records demonstrate similarity in both the average level of the SMB values and inter-annual variability, the coefficient of correlation between them is not significant (0.23 ± 0.19) due to the relatively large amount of noise in the pit record (SNR is about 0.4). However, after smoothing with a 3-year running mean filter, the two time series show a significant correlation ($R = 0.59 \pm 0.16$).

This result, being consistent with the data presented in Fig. 4, supports the validity of the stacked snow accumulation records obtained from multiple snow pit studies, provided the number of pits involved is large enough to significantly reduce the amount of depositional (stratigraphic) noise.

Based on the combined SMB dataset from snow pits and stake farms presented in Fig. 8b, we may conclude that the snow accumulation rate at Vostok has experienced statistically significant decadal variability over the past 80 years:

- Between the mid-1940s and late 1970s, the SMB increased from 18.0 to $23.5 \text{ kg m}^{-2} \text{ yr}^{-1}$.
- During the next two decades, the snow accumulation rate slowed down to an average of $18.2 \text{ kg m}^{-2} \text{ yr}^{-1}$ in the late 1990s.
- Then, in ~ 1999 , a sharp shift in the SMB occurred towards the higher values, and the last two decades were characterized by a rapid increase in the snow accumulation rate, with an average SMB of $25.2 \text{ kg m}^{-2} \text{ yr}^{-1}$ in 2021.

The mean snow accumulation rate in 1970–2021 from the stake farm data is $22.5 \pm 0.3 \text{ kg m}^{-2} \text{ yr}^{-1}$ (± 2 SEM). The minimum and maximum annual SMB values are, respectively, $07.1 \text{ kg m}^{-2} \text{ yr}^{-1}$ (1997) and $31.0 \text{ kg m}^{-2} \text{ yr}^{-1}$ (2004). Thus, the interannual variability of the SMB at Vostok appears to be very strong, with a four-fold difference between the extremes. The mean linear trend of the SMB during the period of observation is $0.03 \text{ kg m}^{-2} \text{ yr}^{-2}$.

4.4. The relationship between the SMB, local air temperature and the Southern Hemisphere climate

In Fig. 8, we compare the Vostok SMB time series with the instrumental record of the 2 m air temperature as observed at the Vostok meteorological station (1958–2020). The correlation coefficient between the two series (0.44 ± 0.13) is statistically significant with $p < 0.005$. The correlation is observed in both the individual annual anomalies and the decadal trends.

In particular, the temperature curve (Fig. 8a) reveals similar decadal variability to the SMB record (Fig. 8b):

- From the late 1950s to late 1970s, the temperature increases from -55.6 to -55.1°C .
- Then, during the next two decades, cooling is observed, down to an average temperature of -56.0°C .
- In the late 1990s, a sharp warming by about 0.7°C occurs, followed by further gradual warming up to -54.0°C in 2020.

Overall, since 1958, the Vostok air temperature increased by about 1.6°C with a particularly strong rate of warming (about 0.6°C per decade) during the last 20 years. Superimposed on this decadal variability are significant interannual oscillations with a SD of 1.0°C . The absolute magnitude of the mean annual 2-m air temperature is 4.4°C (between -57.3 and -52.9°C).

In individual years, anomalies in snow accumulation often correspond to anomalous air temperature: reduced accumulation in 1979, 1997, 2012 and 2019 took place during relatively cold years, while increased accumulation in 1980, 1991, 2014 and 2018 occurred in years warmer than average.

Thus, our instrumental data confirms that local air temperature is the main factor governing the SMB in central Antarctica

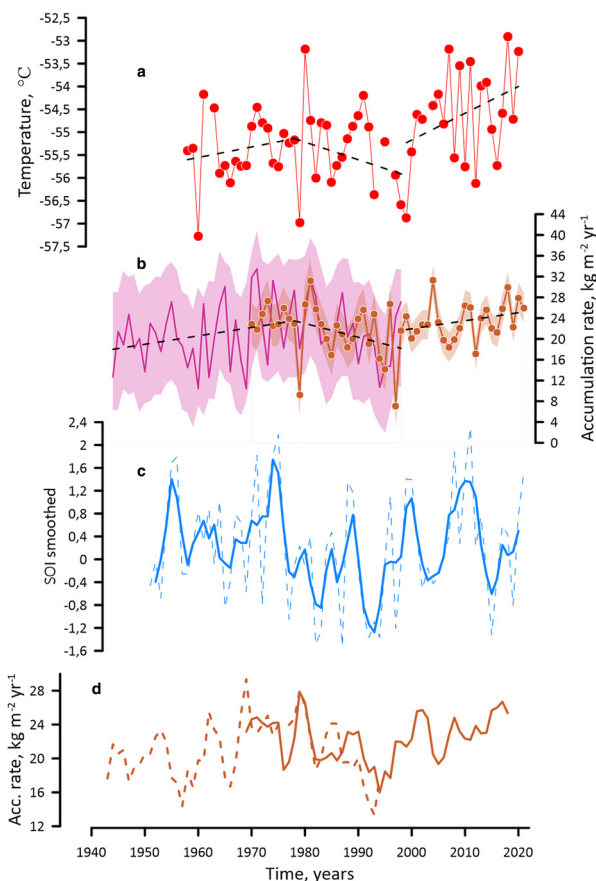


Figure 8. Vostok snow accumulation rate vs local air temperature and Southern Hemisphere climate: (a) mean annual 2 m air temperature as observed at the Vostok meteorological station; (b) composite records of snow accumulation rate from the Vostok stake farms (brown) and from the snow-pit studies (lilac, Ekaykin and others, 2002). The shading depicts the error bars (± 2 SEM). Dashed lines in (a) and (b) are the linear trends of temperature and accumulation rate for the time intervals 1945–1978, 1978–1999 and 1999–2021; (c) mean annual values of SOI (dashed line) and their 3-year running means (solid line); (d) 3-year running means of the Vostok SMB record obtained at the stake farms (solid line) and from the pits (dashed line) shifted by -2 years.

(Frieler and others, 2015). The sensitivity of the snow accumulation rate to the changes of the 2 m air temperature is $2.1 \text{ kg m}^{-2} \text{ yr}^{-1} \text{ K}^{-1}$, or about 9.6% of SMB per K, as calculated using the individual annual values. A similar coefficient ($2.6 \text{ kg m}^{-2} \text{ yr}^{-1} \text{ K}^{-1}$, or 12% of SMB per K) is obtained if we consider linear trends of temperature and the SMB between 1999 and 2021.

According to the published data, the sensitivity of the snow accumulation rate to air temperature in Antarctica is within a range of 3.7 to 13% K^{-1} (see review in the study by Frieler and others, 2015), which is based mainly on the general circulation model simulations. In particular, for Vostok, the sensitivity is $5.9\% \text{ K}^{-1}$ based on data from the ice core and $6.1 \pm 2.5\% \text{ K}^{-1}$ based on the community climate system model (CCSM3) calculations (Frieler and others, 2015). Thus, we conclude that our estimate of the accumulation-temperature sensitivity is within the range of typical values for Antarctica, but slightly higher than that was previously reported for Vostok (Frieler and others, 2015).

We also attempted a comparison of the Vostok SMB time series with the indices of the Southern Hemisphere climate. In particular, it has been previously reported that the Southern Annular Mode (SAM) modulates the precipitation amount over Antarctica (e.g. Marshall and others, 2017). However, the Vostok instrumental SMB record does not demonstrate any correlation with the SAM index, neither for raw nor for smoothed values. Similarly, no correlation was found between the SMB and the Southern Hemisphere sea surface temperature (SST) record or the Indian Ocean SST anomaly, all of which can be considered as proxies for the Vostok moisture source SST.

It was shown previously (Ekaykin and others, 2014) that the Vostok SMB covariates with the Southern Oscillation Index (SOI). The new SMB record presented here confirms this relationship. The anomalies of the snow accumulation rate follow those of the SOI with a lag of 0–3 years (Fig. 8c). For example, the low SMB in 1979 follows the 1977 El Niño event, while the 1997 low SMB coincides with the El Niño event of the same year. The best correlation between the stake-based SMB time series and SOI is observed for the lag of 2 years and for the series smoothed by a 3-year running mean filter ($R = 0.40 \pm 0.13$). For the combined (stakes and pit) SMB time series (1944–2021), the correlation coefficient is 0.21 ± 0.12 ($p = 0.083$). The nature of this teleconnection between the tropical Pacific and central Antarctica is still poorly understood.

5. Conclusion

This article presents a review of the extensive SMB dataset collected from Vostok Station's accumulation stake farms in central East Antarctica since 1970. This instrumental dataset contains >28 000 individual values of snow build-up and >5600 values of surface snow density.

It has been shown that the parameters of the Vostok stake farms are close to optimal for studying the SMB annually: the size of each stake farm ($1 \times 1 \text{ km}$) exceeds the typical size of the snow relief forms, the distance between adjacent stakes (25 m) is large enough to avoid spatial correlation between neighbouring measurements, the number of stakes (79) is low enough to be processed easily within half a day and yet ensures that we may obtain the mean SMB with an uncertainty of about 10%, thus enabling us to reliably resolve the interannual variability of the snow accumulation rate.

Snow build-up in the studied area is characterized by considerable spatial scatter, which manifests itself in the large relative SD of the measurements (CV is about 0.9) and which results in a significant amount of depositional (stratigraphic) noise in the accumulation time series derived at single points from stakes, snow pits and cores. The SNR in an individual time series is as low as 0.045. To obtain a reasonably accurate annually resolved

SMB record, the data from at least ten points should be averaged. This would reduce the relative standard error of annual accumulations from 90 to about 25%.

The stake data have also allowed us to estimate the probability of accumulation hiatuses, which under present-day conditions at Vostok amounts to $19 \pm 2\%$. This means that the snow accumulated over a 1-year period covers only about 4/5 of the surface and that, on average, 1/5 of the annual layers are missing in the pit and core stratigraphy. A similar result is obtained based on stratigraphic studies in eight snow pits excavated in the vicinity of Vostok (Ekaykin and others, 2002).

The seasonal pattern of snow build-up shows that snow accumulation reaches its maximum during the period of midwinter to early spring. The apparently reduced snow build-up in the warm period of the year is thought to be caused by sublimation and the enhanced compaction of the snow.

Since 1970, the average snow accumulation rate at Vostok has been $22.5 \pm 1.3 \text{ kg m}^{-2} \text{ yr}^{-1}$. Our data suggest an overall increase in the SMB during the last 50 years accompanied by a significant decadal variability. The interannual variations in snow accumulation are strongly related to local air temperature showing a SMB-temperature sensitivity of $2.4 \pm 0.2 \text{ kg m}^{-2} \text{ yr}^{-1} \text{ K}^{-1}$ ($11 \pm 2\% \text{ K}^{-1}$).

We also found a covariation between the Vostok SMB and the Southern Oscillation Index: a negative anomaly in the SMB tends to follow the El Niño years with a 0–3 year lag. Interestingly, we did not find a correlation between the SMB and the Southern Annular Mode, which was previously reported to modulate the Antarctic precipitation rate.

The mass balance data collected in recent years in a broader area around Vostok Station suggest that the SMB measurements at Vostok are representative of at least the southern part of subglacial Lake Vostok, up to 100–150 km north of the station and at least 80–100 km south-west and north-west of the station (Vladimirova and others, 2015).

The results of this study (statistical characteristics of the snow build-up values, SNR in the time series obtained from single points, probability of annual layer hiatus in snow thickness) are in first approximation applicable to the low-accumulation area of the central Antarctic plateau that extends along the main ice divide (from Dome C through Ridge B and Dome A to Dome Fuji).

Data. The meteorological data for Russian Antarctic stations is available at AARI's website: http://www.aari.aq/default_en.html. In the left panel, click 'Summary table' in the 'Meteorology (climate)' section. SOI data are available at the National Oceanic and Atmospheric Administration website: <https://www.ncei.noaa.gov/access/monitoring/enso/soi>. The data from the Vostok stake farms presented here is deposited at Zenodo storage (doi: 10.5281/zenodo.8095516). The same dataset can also be downloaded at the CERL website (<http://cerl-aari.ru/index.php/smb-vostok/>).

Acknowledgements. We are grateful to all the participants of Russian Antarctic Expedition who took part in glaciological works at the Vostok stake farms. The manuscript was substantially improved by constructive comments by Editor Dr Carleen Reijmer and 3 anonymous reviewers. We thank Matthew Lazzara, Takao Kameda and Jean Robert Petit for valuable discussions, and Alice Lagnado for improving the English. We are grateful to Dr Sergey Popov (Polar Marine Geological Research Expedition) who helped us to draw Fig. 1. This work was supported by Russian Science Foundation grant 21-17-00246.

Author contributions. A. E. and V. L. participated in the fieldwork and prepared the manuscript. All authors contributed to the data processing, analysis and interpretation.

References

Agosta C and 10 others (2019) Estimation of the Antarctic surface mass balance using the regional climate model MAR (1979–2015) and identification

- of dominant processes. *The Cryosphere* **13**, 281–296. doi: [10.5194/tc-13-281-2019](https://doi.org/10.5194/tc-13-281-2019)
- Amory C and 6 others** (2021) Performance of MAR (v3.11) in simulating the drifting-snow climate and surface mass balance of Adélie Land, east Antarctica. *Geoscientific Model Development* **14**, 3487–3510. doi: [10.5194/gmd-14-3487-2021](https://doi.org/10.5194/gmd-14-3487-2021)
- Barkov NI and Lipenkov VYa** (1978) Snow accumulation in the vicinity of Vostok Station in 1970–1973. *Information Bulletin of the Soviet Antarctic Expedition* (98), 63–68.
- Del Guasta M** (2022) ICE-CAMERA: a flatbed scanner to study inland Antarctic polar precipitation. *Atmospheric Measurement Techniques* **15**, 6521–6544. doi: [10.5194/amt-15-6521-2022](https://doi.org/10.5194/amt-15-6521-2022)
- DiMarzio J, Brenner A, Schutz R, Shuman CA and Zwally HJ** (2007) *GLAS/ICESat 500 m Laser Altimetry Digital Elevation Model of Antarctica*. Boulder, CO, USA: National Snow and Ice Data Center. Digital Media, vol. **10**, K2IMI0L24BRJ.
- Ding M and 6 others** (2011) Spatial variability of surface mass balance along a traverse route from Zhongshan station to Dome A, Antarctica. *Journal of Glaciology* **57**(204), 658–666.
- Ding M and 8 others** (2016) Re-assessment of recent (2008–2013) surface mass balance over Dome Argus, Antarctica. *Polar Research* **35**(26133), 1–8. doi: [10.3402/polar.v35.26133](https://doi.org/10.3402/polar.v35.26133)
- Dunmire D, Lenaerts JTM, Datta RT and Gorte T** (2022) Antarctic surface climate and surface mass balance in the Community Earth System Model version 2 during the satellite era and into the future (1979–2100). *The Cryosphere* **16**, 4163–4184. doi: [10.5194/tc-16-4163-2022](https://doi.org/10.5194/tc-16-4163-2022)
- Eisen O and 15 others** (2008) Ground-based measurements of spatial and temporal variability of snow accumulation in east Antarctica. *Reviews of Geophysics* **46**(RG2001), 1–39.
- Eisen O, Rack W, Nixdorf U and Wilhelms F** (2005) Characteristics of accumulation around the EPICA deep-drilling site in Dronning Maud Land, Antarctica. *Annals of Glaciology* **41**, 41–46.
- Ekaykin AA and 6 others** (2016) Non-climatic signal in ice core records: lessons from Antarctic mega-dunes. *The Cryosphere* **10**, 1217–1227. doi: [10.5194/tc-10-1217-2016](https://doi.org/10.5194/tc-10-1217-2016)
- Ekaykin AA and 10 others** (2019) Spatial variability of snow isotopic composition and accumulation rate at the stake farm of Vostok Station (central Antarctica) [in Russian]. *Probl. Arktiki i Antarktiki* **65**(1), 46–62. doi: [10.30758/0555-2648-2019-65-1-46-62](https://doi.org/10.30758/0555-2648-2019-65-1-46-62)
- Ekaykin AA and 5 others** (2020) Underestimation of snow accumulation rate in central Antarctica (Vostok Station) derived from stake measurements. *Russian Meteorology and Hydrology* **45**(2), 132–140. doi: [10.3103/S1068373920020090](https://doi.org/10.3103/S1068373920020090)
- Ekaykin AA, Kozachek AV, Lipenkov VYa and Shibaev YuA** (2014) Multiple climate shifts in the Southern Hemisphere over the past three centuries based on central Antarctic snow pits and core studies. *Annals of Glaciology* **55**(66), 259–266.
- Ekaykin AA, Lipenkov VYa and Barkov NI** (1998) Spatial and temporal structure of snow accumulation field in the vicinity of Vostok Station, central Antarctica [in Russian]. *Vestnik SPbGU, Series 7* **4**(28), 38–50.
- Ekaykin AA, Lipenkov VYa, Barkov NI, Petit JR and Masson-Delmotte V** (2002) Spatial and temporal variability in isotope composition of recent snow in the vicinity of Vostok Station: implications for ice-core interpretation. *Annals of Glaciology* **35**, 181–186.
- Ekaykin AA, Zarovchatskiy VN and Lipenkov VYa** (2015) Measurements of snow sublimation rate at Vostok Station (Antarctica) [in Russian]. *Probl. Arktiki i Antarktiki* **4**(106), 20–25.
- Fisher DA, Reeh N and Clausen HB** (1985) Stratigraphic noise in time series derived from ice cores. *Annals of Glaciology* **7**, 76–83.
- Frederikse T and 6 others** (2020) Antarctic ice sheet and emission scenario controls on 21st-century extreme sea-level changes. *Nature Communications* **11**(390), 1–11. doi: [10.1038/s41467-019-14049-6](https://doi.org/10.1038/s41467-019-14049-6)
- Frieler K and 8 others** (2015) Consistent evidence of increasing Antarctic accumulation with warming. *Nature Climate Change* **5**, 348–352. doi: [10.1038/NCLIMATE2574](https://doi.org/10.1038/NCLIMATE2574)
- Genthon C, Six D, Sarchilli C, Ciardini V and Frezzotti M** (2016) Meteorological and snow accumulation gradients across Dome C, east Antarctic plateau. *International Journal of Climatology* **36**(1), 455–466. doi: [10.1002/joc.4362](https://doi.org/10.1002/joc.4362)
- Hamilton GS** (2004) Topographic control of regional accumulation rate variability at South Pole and implications for ice-core interpretation. *Annals of Glaciology* **39**, 214–218.
- Ismagilov NV, Aukhadeev TR and Tudriy VD** (2018) Methods and equipment of hydrometeorological measurements [in Russian]. In Sabirova MV and Sharifullin AG eds. *Methodical Guidebook*. Kazan: Kazan Univ. Press.
- Kameda T, Motoyama H, Fujita S and Takahashi S** (2008) Temporal and spatial variability of surface mass balance at Dome Fuji, east Antarctica, by the stake method from 1995 to 2006. *Journal of Glaciology* **54**(184), 107–116.
- Lazzara MA, Keller LM, Markle T and Gallagher J** (2012) Fifty-year Amundsen–Scott South Pole station surface climatology. *Atmospheric Research* **118**, 240–259. doi: [10.1016/j.atmosres.2012.06.027](https://doi.org/10.1016/j.atmosres.2012.06.027)
- Marshall GJ, Thompson DWJ and van den Broeke M** (2017) The signature of Southern Hemisphere atmospheric circulation patterns in Antarctic precipitation. *Geophysical Research Letters* **44**, 11580–11589. doi: [10.1002/2017GL075998](https://doi.org/10.1002/2017GL075998)
- Medley B and Thomas ER** (2019) Increased snowfall over the Antarctic ice sheet mitigated twentieth-century sea-level rise. *Nature Climate Change* **9**, 34–41. doi: [10.1038/s41558-018-0356-x](https://doi.org/10.1038/s41558-018-0356-x)
- Meredith M and 12 others** (2019) Polar regions. In Pörtner H-O, Roberts DC, Masson-Delmotte V, Zhai P, Tignor M, Poloczanska E, Mintenbeck K, Alegria A, Nicolai M, Okem A, Petzold J, Rama B and Weyer NM (eds), *IPCC Special Report on the Ocean and Cryosphere in a Changing Climate*. Cambridge and NY: Cambridge University Press, pp. 203–320. doi: [10.1017/9781009157964.005](https://doi.org/10.1017/9781009157964.005)
- Mottram R and 16 others** (2021) What is the surface mass balance of Antarctica? An intercomparison of regional climate model estimates. *The Cryosphere* **15**, 3751–3784. doi: [10.5194/tc-15-3751-2021](https://doi.org/10.5194/tc-15-3751-2021)
- Petit JR, Jouzel J, Pourchet M and Merlivat L** (1982) A detailed study of snow accumulation and stable isotope content in Dome C (Antarctica). *Journal of Geophysical Research* **87**(C6), 4301–4308.
- Picard G, Arnaud L, Caneill R, Lefebvre E and Lamare M** (2019) Observation of the process of snow accumulation on the Antarctic Plateau by time lapse laser scanning. *The Cryosphere* **13**, 1983–1999. doi: [10.5194/tc-13-1983-2019](https://doi.org/10.5194/tc-13-1983-2019)
- Popov SV and Masolov VN** (2007) Forty-seven new subglacial lakes in the 0–110°E sector of east Antarctica. *Journal of Glaciology* **53**(181), 289–297.
- Richter A and 8 others** (2021) Surface mass balance models vs. stake observations: a comparison in the Lake Vostok region, central east Antarctica. *Frontiers in Earth Science* **9**(669977), 1–14. doi: [10.3389/feart.2021.669977](https://doi.org/10.3389/feart.2021.669977)
- Shen X, Ke C-Q, Fan Y and Drolma L** (2022) A new digital elevation model (DEM) dataset of the entire Antarctic continent derived from ICESat-2. *Earth System Science Data* **14**, 3075–3089. doi: [10.5194/essd-14-3075-2022](https://doi.org/10.5194/essd-14-3075-2022)
- Slater T, Hogg AE and Mottram R** (2020) Ice-sheet losses track high-end sea-level rise projections. *Nature Climate Change* **10**, 877–881. doi: [10.1038/s41558-020-0893-y](https://doi.org/10.1038/s41558-020-0893-y)
- Sorge E** (1935) Glaziologische Untersuchungen in Eismitte. *Wissenschaftliche Ergebnisse der Deutschen Groenland-Expedition Alfred Wegener 1929 und 1930/1931*. Leipzig: F.A. Brockhaus, 62–270.
- Takahashi S and Kameda T** (2007) Snow density for measuring surface mass balance using the stake method. *Journal of Glaciology* **53**(183), 677–680.
- Thomas ER and 15 others** (2017) Regional Antarctic snow accumulation over the past 1000 years. *Climate of the Past* (13), 1491–1513. doi: [10.5194/cp-13-1491-2017](https://doi.org/10.5194/cp-13-1491-2017)
- Turner J and 12 others** (2019) The dominant role of extreme precipitation events in Antarctic snowfall variability. *Geophysical Research Letters* **46**(6), 3502–3511. doi: [10.1029/2018GL081517](https://doi.org/10.1029/2018GL081517)
- van der Veen CJ, Mosley-Thompson E, Gow A and Mark BG** (1999) Accumulation at South Pole: comparison of two 900-year records. *Journal of Geophysical Research* **104**(D24), 31067–31076.
- van Wessem JM and 6 others** (2018) Modelling the climate and surface mass balance of polar ice sheets using RACMO2 – part 2: Antarctica (1979–2016). *The Cryosphere* **12**, 1479–1498. doi: [10.5194/tc-12-1479-2018](https://doi.org/10.5194/tc-12-1479-2018)
- Vladimirova DO, Ekaykin AA, Lipenkov VYa, Popov SV and Shibaev YuA** (2015) Spatial variability of the accumulation rate and isotopic composition of the snow in Indian Ocean sector of east Antarctica including the vicinity of subglacial Lake Vostok [in Russian]. *Probl. Arktiki i Antarktiki* **103**(1), 69–86.